Dynamic trajectory for landing an aerial vehicle on a mobile platform.

A. Alatorre, J. Cariño, Pedro Castillo Garcia, Rogelio Lozano

Dynamic trajectory for landing an aerial vehicle on a mobile platform.

A. Alatorre, *,** **J. Cariño,** * **P. Castillo,** * **R. Lozano.** *,**

* *Heuristics and Diagnosis of Complex Systems, CS 60319 - 60203 Compiègne Cedex, France. Emails: (castillo, rlozano, aalatorr)@hds.utc.fr and jcarinoe@hds.utc.fr.*
** *Center of Research and Advanced Studies of the National Polytechnic Institute (CINVESTAV), Mexico.*

Abstract: In the presented work, a trajectory is designed allowing an Unmanned Aerial Vehicle (UAV) to perform landing on a mobile platform. The proposed trajectory behaves in such a way that grants a seamless integration of information about the target landing platform into its design. This allows any generic tracking controller to follow the trajectory regardless of the target's dynamics or movement, as they are indirectly applied to the trajectory's architecture. The focus of this work is for fixed-wing aircraft to land on water surface vehicles but can be adjusted for different scenarios. One of which is used for the experimental corroboration of the proposed strategy in a real-world environment.

Keywords: Autonomous landing, dynamic trajectory, rendevous, target following, UAV.

1. INTRODUCTION

Researches into Unmanned Aerial Vehicles (UAV) have explored solutions in several application domains, such as the path planning for photogrammetry (Cabreira et al, 2018), guidance strategies for ground reconnaissance (Iscold et al, 2010), target detection for search-rescue (Sun et al, 2016), control design for tracking of ground vehicles (Oliveira & Encarnação, 2013), parameter estimators for payloads transportation (Wang et al, 2016), and the design of adaptive control to navigate in presence of wind disturbances (Brezoescu et al, 2013).

UAVs are commonly classified as multirotor or fixed-wing vehicles. A multirotor vehicle is comprised of more than two rotors, and is capable of vertical take-off and landing, (Castillo et al, 2006). Besides, thanks to its vertical thrust, the vehicle can remain at hover flight and perform high-precision maneuvers. However, this kind of drone presents a low performance when flying long distances, going at high speeds, and very small flight durability.

Alternatively, a fixed-wing vehicle can achieve the previous tasks seamlessly, as is mentioned in (Varga et al, 2015). Since the lift force is generated by the airflow through of its wings when the vehicle moves forward. This allows the airplane to glide without taxing the engine too much. Thus, it is a suitable vehicle to perform long-distance missions with low energy consumption, (Elijah et al, 2021).

Although, landing is a critical flight stage for fixed-wing drones. Often, they suffer accidents caused by the inexperience of pilots or by crosswind disturbances, (Huh & Shim, 2010). Therefore, some research has been carried out to achieve automatic landing to reduce the accident numbers.

⋆ This paper was supported by the RPV project - UTC foundation and the Mexican National Council of Science and Technology - CONACyT.

The authors in (Zhang & Wang, 2017) define the automatic landing for a fixed-wing vehicle on a runway in three flight stages: descent, flare maneuver, and taxiing for kinetic energy reduction. The challenge of an automatic landing increases when the place to land is a moving target, as any error or miscalculation could result in a failure.

The goal is to develop a dynamic trajectory to facilitate the landing task on a moving target. Besides providing a safe landing solution for UAV's without landing gear such as in (Muskardin et al, 2016). The proposed strategy can be used along a suitable tracking controller that might already be implemented on the UAV.

The literature has previously presented strategies for leading a vehicle towards a target. Among these, two remain popular to address the proposed situation: Dynamic Path Following (DPF); and Rendezvous Guidance Control.

DPF is a strategy that steers a vehicle towards a trajectory, which is based on a moving target. An autonomous vehicle is often defined as the target where all its states can be known by the follower, (Reis et al, 2019).

The rendezvous control works with the differential geometry method. This method focuses on the angular difference between the target and the follower, (Oh et al, 2013).

Comparing the strategies, rendezvous approach, using a control based on differential geometry, is a method more complex than the dynamic path following since the last method can be addressed to a trajectory tracking problem.

In this work, we propose a landing dynamic trajectory to guide an aerial vehicle towards the target position at a certain rendezvous longitude, l_R. The desired trajectory depends on the target position, which is the path parameter that provides the evolution of a descending slope until the target is reached.

The manuscript is organized as follows: the mathematical preliminaries are defined in Section 2. The problem statement is given in Section 3. The landing dynamic trajectory is defined in Section 4. The motion equations and control strategy for a fixed-wing drone are described in Section 5. An experimental validation is developed using a quadcopter for the trajectory evaluation. The quadcopter control strategy is described in Section 6. Landing trajectory performance is corroborated by the results of simulations and experiments in Section 7. Finally, concluding remarks and future research directions are presented in Section 8.

2. PRELIMINARIES

2.1 Quaternion modeling

Quaternion definitions The quaternion set is described as $\mathbb{H}$. A single quaternion variable $\boldsymbol{q} := q_0 + \overrightarrow{q} \in \mathbb{H}$ can be considered as a four tuple with one scalar part $q_0 \in \mathbb{R}$ and the sum of three imaginary parts $q_1, q_2, q_3 \in \mathbb{R}$ using three unit imaginary perpendicular vectors $\boldsymbol{i}, \boldsymbol{j}, \boldsymbol{k} \in \mathbb{R}^3$. This last one can be summarized using the following notation: $\overrightarrow{q} = q_1\,\boldsymbol{i} + q_2\,\boldsymbol{j} + q_3\,\boldsymbol{k}$ as described in (Kuipers, 1999). A quaternion can be represented using the following four tuple in vector form

$$\mathbf{q} = [q_0,\ \overrightarrow{q}]^T. \tag{1}$$

The main operation for a quaternion is the product, which is defined using vector operations for two quaternions $\boldsymbol{q}, \boldsymbol{r} \in \mathbb{H}$ as:

$$\boldsymbol{q} \otimes \boldsymbol{r} := (q_0\, r_0 - \overrightarrow{q} \cdot \overrightarrow{r}) + (q_0\, \overrightarrow{r} + r_0\, \overrightarrow{q} + \overrightarrow{q} \times \overrightarrow{r}), \tag{2}$$

where $\cdot$ and $\times$ are the vector inner and outer products.

Vectors in 3D space can be considered as quaternions with null scalar parts, which are also called pure quaternions. It can be seen from equation (2) that the quaternion product is compatible with 3D vectors.

A useful linear operation, akin to complex numbers, is the quaternion conjugate:

$$\boldsymbol{q}^* := q_0 - \overrightarrow{q}. \tag{3}$$

The quaternion norm can be defined as :

$$\|\boldsymbol{q}\| := \boldsymbol{q} \otimes \boldsymbol{q}^* = q_0^2 + q_1^2 + q_2^2 + q_3^2. \tag{4}$$

A quaternion with unitary norm $\|\boldsymbol{q}\| = 1$ is called a unitary quaternion, and these are the ones used for the description of the attitude in a rigid body.

An operation that will be later used is the quaternion natural logarithm function, which is described for a unit quaternion $\boldsymbol{q} \in \mathbb{H}, \|\boldsymbol{q}\| = 1$ as

$$\log \boldsymbol{q} := \begin{cases} \dfrac{\overrightarrow{q}}{\|\overrightarrow{q}\|} \arccos q_0, & \|\overrightarrow{q}\| \neq 0 \\ 0, & \|\overrightarrow{q}\| = 0 \end{cases} \tag{5}$$

Attitude representation using quaternions The rotation operation of a 3D vector $\overrightarrow{v} \in \mathbb{R}^3$ from one reference frame into another $\overrightarrow{v} \rightarrow \overrightarrow{v}'$ can be described using an unitary quaternion $\boldsymbol{q} \in \mathbb{H}$ by means of the Euler-Rodrigues formula, (Morais, 2014):

$$\overrightarrow{v}' := \boldsymbol{q} \otimes \overrightarrow{v} \otimes \boldsymbol{q}^* \tag{6}$$

where the quaternion is calculated as

$$\boldsymbol{q} := \cos\left(\frac{\theta}{2}\right) + \overrightarrow{n}\,\sin\left(\frac{\theta}{2}\right) \tag{7}$$

where $\theta \in \mathbb{R}$ is a rotation quantity and $\overrightarrow{n} \in \mathbb{R}^3$ is a unit 3D vector that marks the axis of rotation.

In the particular case of rigid bodies, the equations (6) and (7) can be used as a means to describe the full attitude of the object.

3. PROBLEM STATEMENT

The objective is to design a strategy to land on a mobile target. In our case, it is assumed that a suitable tracking controller has already been implemented and is able to track a desired trajectory without issues. This also implies that the associated perturbations due to the moving platform are absorbed by the control law.

The focus therefore shifts towards the design and corroboration of a suitable trajectory for the tracking control algorithm that would allow an UAV to safely land on a mobile target. The proposed UAV is a fixed-wing vehicle, but the strategy could be adapted to more agile vehicles. An advantage that the drone has is that it is assumed that the full state of the landing platform is always known.

4. LANDING DYNAMIC TRAJECTORY

The design of the reference trajectory is based on two techniques. The first one is the dynamic path following, that consists of steering an autonomous vehicle toward a geometric trajectory defined by the target's motion. The second strategy is named glide path, which is defined as a straight line directed to the landing point.

As mentioned, the desired trajectory focuses on leading the fixed-wing drone towards the position of a moving target in the x-z plane. A ground vehicle is defined as the target.

The coordinate system related to the inertial frame is denoted by $\{I\}$. The body frame of the follower vehicle is defined by $\{B\}$, and the target frame by $\{T\}$. The position vectors of the vehicles' center of mass are defined in $\{I\}$, where $(x_T,\, z_T)$ represents the target position, and $(x,\, z)$ denotes the follower position. Figure 1 shows a diagram of the proposed trajectory.

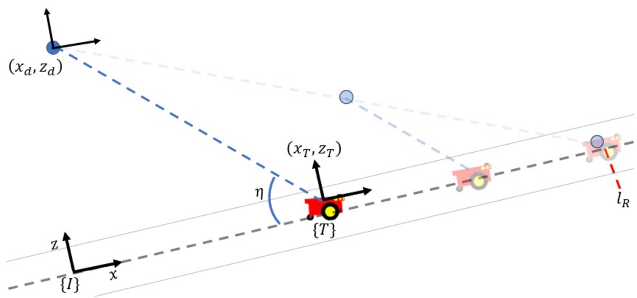

Fig. 1. Landing dynamic trajectory scheme.

The landing dynamic trajectory develops a descending flight based on a slope directed to the target. The trajectory is a function of the target displacement, this parameter path reduces the slope's distance between the desired position and the target, keeping an $\eta \in \mathbb{R}$ constant angle, see Figure 2. Moreover, this figure shows the association between the desired position and the target's position using reference circles.

Therefore, the fixed-wing vehicle tracks the trajectory and it will reach the target's position after the target navigates a defined longitude denoted by $l_R \in \mathbb{R}_+$. The $l_R \in \mathbb{R}_+$ path parameter represents the rendezvous point between the trajectory and the target, that is, $x_d = x_T = l_R$.

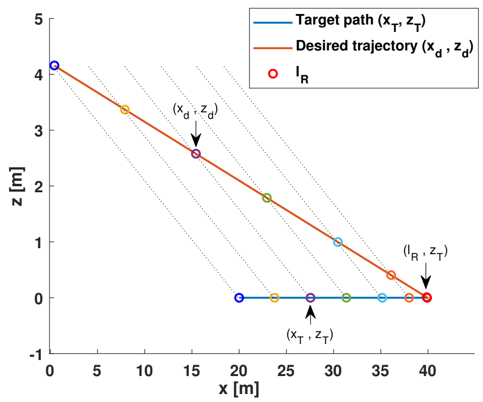

Fig. 2. Study of the desired trajectory behavior, to reach the target position.

The desired trajectory is defined as:

$$x_d = x_T - (l_R - x_T)\cos\eta, \tag{8}$$

$$z_d = z_T + (l_R - x_T)\sin\eta. \tag{9}$$

In addition, the desired velocities of the trajectory can be calculated as follows

$$\dot{x}_d = \dot{x}_T(1 + \cos\eta), \tag{10}$$

$$\dot{z}_d = -\dot{x}_T \sin\eta. \tag{11}$$

This allows to implement different control techniques to carry out the trajectory tracking as the information of the speed of the target is available.

5. SIMULATION FOR A FIXED-WING DRONE

The following section describes the longitudinal model of a fixed-wing UAV and the corresponding tracking controller design that were used to validate the proposed trajectory using numerical simulations.

5.1 Longitudinal motion equations for a fixed-wing drone

A reduced-order longitudinal guidance model for a fixed-wing drone can be written as in (Beard & McLain, 2012), it is described as follows:

$$\dot{x} = V_a \cos\gamma \tag{12}$$

$$\dot{z} = V_a \sin\gamma \tag{13}$$

$$\dot{\gamma} = \frac{F_L}{mV_a} - \frac{g}{V_a}\cos\gamma, \tag{14}$$

where $(x,\ z)$ represents the aircraft's position defined in the inertial frame. γ describes the flight path angle, and V_a denotes the airspeed, which is defined as a constant value. The terms m and g are the mass and the acceleration due to the gravity, respectively. This model comprises a combination of kinematic and dynamic equations. Moreover, it considers that the angle of attack $\alpha \approx 0$. Therefore, the F_L lift force can be written of the following form:

$$F_L = \frac{1}{2}\rho V_a^2 S_a [C_{L0} + C_{D_{\delta_e}} \delta_e] \tag{15}$$

The air density is denoted by ρ, and S_a defines the surface area of the wing. Finally, the control input involved in the lift force is the elevator's deflection, which is depicted by δ_e. Notice that equations (15) involves the relations with the lift coefficients, they are defined by the features of each aircraft.

5.2 Tracking controller design for a fixed-wing drone

The design of the control law to follow the desired trajectory are corroborated using Lyapunov stability analysis. We will present the strategy to track the desired positions trajectory. Considering the aircraft dynamics, the aircraft will be guided based on a desired flight path angle, which is denoted by γ_d.

From Figure 3, the desired flight angle can be calculated through

$$\gamma_d = \tan^{-1}\left(\frac{z_d - z}{x_d - x}\right), \tag{16}$$

and its derivative is given by

$$\dot{\gamma}_d = -\frac{(x_d - x)\left[\dot{z}_d + \dot{z} + \Delta(\dot{x}_d - x)\right]}{(x_d - x)^2 + (z_d - z)^2}, \tag{17}$$

where

$$\Delta = \frac{z_d - z}{x_d - x}. \tag{18}$$

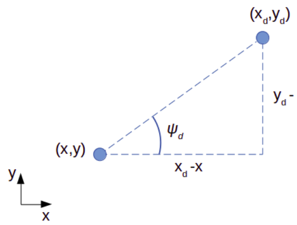

Fig. 3. Representation of the reference angle.

Defining the tracking error as $e_\gamma = \gamma - \gamma_d$. We propose a positive function $V_1 = \frac{1}{2}e_\gamma^2$, differentiating and substituting (14), it follows

$$\dot{V}_1 = e_\gamma\left(\frac{F_L}{mV_a} - \frac{g}{V_a}\cos\gamma - \dot{\gamma}_d\right) < 0. \tag{19}$$

Therefore, it is possible to solve the equation for the elevator control input δ_e, whose result can be defined as

$$\delta_e = -\frac{V_a}{C_{L_{\delta_e}}} + \frac{2m}{\rho V_a^2 S_a C_{L_{\delta_e}}}\left[g\cos\gamma + \dot{\gamma}_d - V_a e_\gamma\right]. \tag{20}$$

Introducing (20) into (19), then $\dot{V}_1 = -e_\gamma^2$, that is, $\gamma \to \gamma_d$.

6. EXPERIMENTAL VALIDATION USING A QUADCOPTER VEHICLE

The real-time implementation of our landing dynamic trajectory on a real-world platform will validate its performance and viability. Since the main advantage is the facility of implementation and the dependency on the movement of the target. The strategy is designed to guide one aerial vehicle towards a rendezvous point, reaching the target's position. The experimental validation is performed in an indoor environment using a quadcopter ARDrone 2.

The original firmware of this drone was replaced by the open-source software Fl-AIR (Framework Libre AIR), which takes an important roll to integrate the quadcopter with the localization system and is described in more detail in (Sanahuja, 2012).

In addition, a ground vehicle, Parrot Jumping Sumo, is used as a target. It is controlled manually by a pilot. The interchange of data between target-follower is available such as the target's position and speed, which is obtained by an OptiTrack motion capture system.

The control strategy used to track the trajectory in the test is described in the following section.

6.1 Quadcopter control strategy

The model and the control strategy used for the quadcopter vehicle has been discussed in detail in (Carino, 2015). The model is out of the scope of this work, but the control will be briefly discussed to show how to implement the trajectory tracking. Basically, an inner position control gives a reference to an outer attitude control.

The position control is defined for the tracking of the proposed trajectory as :

$$\vec{u}_{pos} := -K_{pos}\,\vec{E} - K_{vel}\,\dot{\vec{E}}. \tag{21}$$

where $\vec{E}$ represents the tracking error vector given by

$$\vec{E} := [(x - x_d)\,,\,(z - z_d)]^T, \tag{22}$$

K_{pos} and K_{vel} depict the gains matrices of position and velocity. The attitude control is defined as :

$$\vec{u}_{att} := -2\,K_{att}\,\ln \boldsymbol{q}_e - k_\omega\,\vec{\omega}, \tag{23}$$

K_{att} is the attitude gains, $\vec{\omega}$ depicts the angular velocity vector, and the quaternion attitude error $\boldsymbol{q}_e \in \mathbb{H}$ defines as:

$$\boldsymbol{q}_e := \boldsymbol{q}_d^* \otimes \boldsymbol{q}. \tag{24}$$

The attitude of the vehicles is depicted by the unit quaternion $\boldsymbol{q}$ and the desired quaternion $\boldsymbol{q}_d$ is defined using the position control (21) as :

$$\begin{aligned} \boldsymbol{q}_d' &:= \left(\vec{b}\cdot\vec{u}_{pos} + \|\vec{u}_{pos}\|\right) + \vec{b}\times\vec{u}_{pos} \\ \boldsymbol{q}_d &:= \frac{\boldsymbol{q}_d'}{\|\boldsymbol{q}_d'\|} \end{aligned} \tag{25}$$

where $\vec{b}$ depicts a unitary vector denoting the axis in which the thrust acts in $\{B\}$. Therefore, the control input for the quadcopter platform is the attitude control torques as described in (23) and the scalar thrust

$$u_{thrust} := \|\vec{u}_{pos}\| \tag{26}$$

The combination of both of these strategies allows for the successful tracking of the proposed trajectory in a quadcopter vehicle. This can be corroborated in practice by measuring the distance between the desired trajectory and the quadcopter's position.

7. RESULTS

7.1 Simulation results for the fixed-wing aerial vehicle

The landing dynamic trajectory is implemented and validated in a Simulink simulations, using the solver 0de4 (Runge-Kutta) with a sample time of 0.001 s.

The aerodynamic parameters of the fixed-wing drone are obtained in (Alatorre et al, 2021). As mentioned, a ground vehicle is defined as the target with an altitude of 0.5 meters and a velocity $\dot{x}_T = 2$ m/s.

The goal is to validate the landing dynamic trajectory since it guides the aircraft towards the target position. The rendezvous position is defined in $(l_R, z_T) = (10, 0.5)$ m. Moreover, the desired trajectory angle is given by $\eta = 12°$.

The initial position of the target vehicle is defined in $(x_T(0), z_T(0)) = (0, 0)$ m and the initial position of the fixed-wing drone is given by $(x(0), z(0)) = (-14, 2.5)$ m. The airspeed of the drone is defined by 5 m/s.

Figure 4 shows the simulation result of tracking the landing trajectory. The navigation path of the target is depicted by the green line, the landing dynamic trajectory is defined as the red line, and the path of the fixed-wing drone is depicted by the blue line.

Notice that the drone performs a descending flight, reaching the desired trajectory. The trajectory evolves with an η constant angle, and the distance between $(x_d,\, z_d)$ and $(x_T,\, z_T)$ reduces until reaching the target position.

The target vehicle navigates in a straight line until l_R where the drone converges to the target position such as is shown in the zoom of the Figure 4.

Considering the elevator control input (20), the flight path angle tracks to the desired angle given in (16). Therefore, we can observe the behavior of γ to reach γ_d in Figure 5. The above leads to the aircraft towards the target position.

We compute the $||\vec{E}||$ norm to be shown in a logarithmic form in Figure 6. As result, $||\vec{E}|| \to 0$.

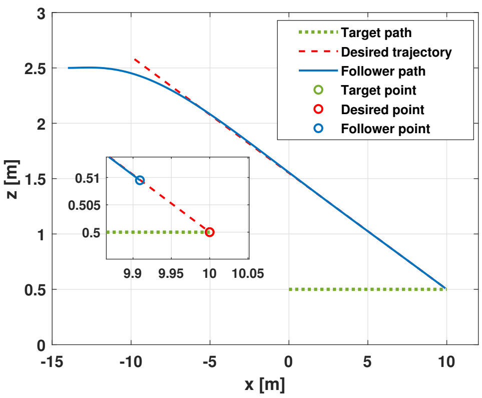

Fig. 4. Trajectory tracking using a fixed-wing drone.

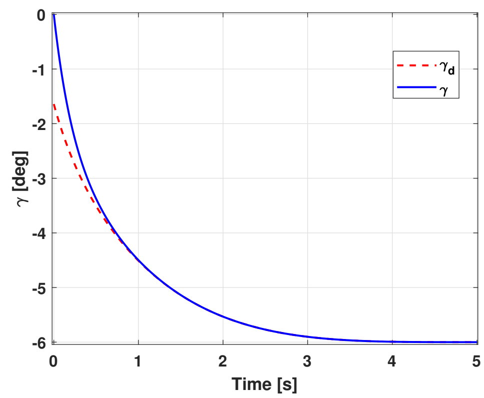

Fig. 5. Behavior of the flight path angle.

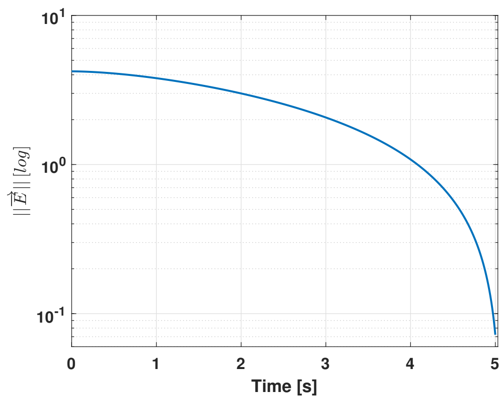

Fig. 6. Norm of the tracking errors.

7.2 Experimental results

In this section, we present the experimental results of the landing dynamic trajectory using a quadcopter vehicle. The experimental flight test is initially defined by keeping the drone at hover flight at the initial desired altitude.

Since the target has less dimension than the drone, we define z_T with the height of a landing platform. It will be located in the rendezvous point, *i.e.* at the position of l_R.

The experiment stages are described as follows:

- The target is located in the origin of flight room.
- The quadcopter takes-off and keeps a hover flight on the initial position of $(x_d \, , \, z_d)$.
- The ground vehicle navigates in a straight line towards the landing platform.
- The drone's controller tracks the trajectory and finally lands on the platform.

The desired trajectory parameters were fixed in order to accommodate the available flight space.

Table 1. Experimental Parameters

Parameters	Value	Units
η	$50°$	degrees
l_R	3	meters
z_T	0.5	meters
$x_T(0)$	0	meters
$(x(0), z(0))$	$(-2, 2.7)$	meters

A video of the experimental validation of the landing dynamic trajectory can be seen at:

https://youtu.be/UxMJNoK_VJ4

Figure 7 shows the performance of the desired trajectory related to the target's movement. Observe that the drone starts the mission at hover. Then, it executes the trajectory tracking algorithm where we note that the drone's path approximates to the trajectory. The target is illustrated in the zoom of Figure 7. It can be clearly seen that the drone approximates to the target position with a minimum error.

On one hand, we can visualize in Figure 8 how the displacement in the x axis of the target vehicle influences the behavior of the desired position x_d. This forces the aircraft to navigates until the x_T position. On the other hand, the desired altitude tends to decrease as the target vehicle moves towards the rendezvous point, see Figure 9. Therefore, the quadcopter also reduces gradually its altitude with respect to the desired altitude, which implies landing on the target.

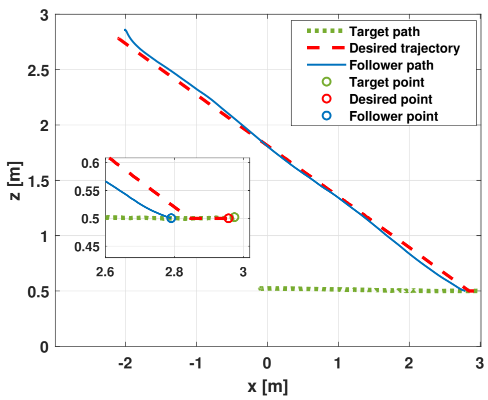

Fig. 7. Experimental result of the landing dynamic trajectory executed by a quadcopter vehicle.

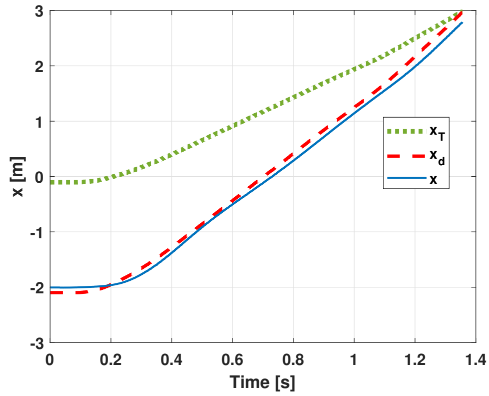

Fig. 8. Performance of the desired path based on the target displacement in the x-axis.

Finally, we compute the norm of the tracking error vector, which is defined in (22). We obtain that $||\overrightarrow{E}||$ is a minimum value which approximates to zero, which is represented in logarithm scale in the Figure 10.

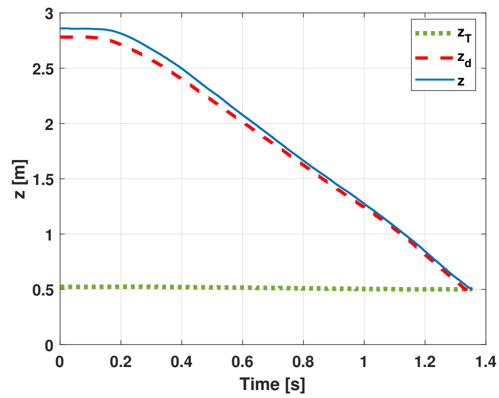

Fig. 9. Behavior of the desired altitude imposing a descending flight for a quadcopter.

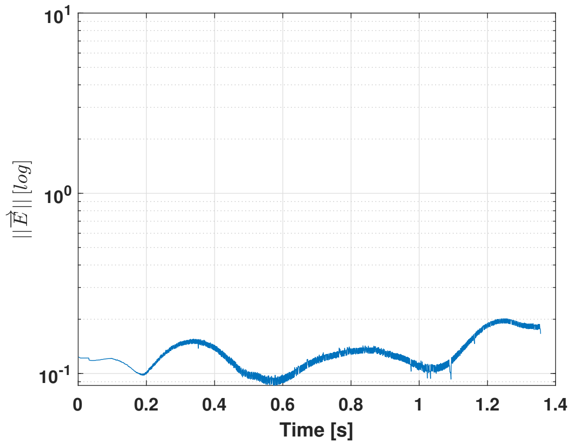

Fig. 10. Result of the normalized tracking error in the experimental flight.

8. CONCLUSION

In this paper, a landing dynamic trajectory was presented, designed and tested to guide an aerial vehicle towards the position of a mobile target. The convergence of the position between the vehicles is achieved after the target navigates to reach a predefined distance.

The validation of the landing dynamic trajectory was made using simulations and experiments. The simulation results clearly show that a fixed-wing vehicle would be able to land on a mobile target using the proposed trajectory. The constant angle of the trajectory allows to adapt to the speed and distance towards the target just before starting the tracking. Once engaged, the proposed controller shows how the tracking error diminishes as time advances even with the movement of the target.

In the experimental results, it was proven that the implemented control strategy was successful in tracking the desired trajectory in a real-world scenario. The low error implies that the quadcopter was practically always following the trajectory. The video also demonstrates how this design could be used to land an aerial vehicle on a moving target.

8.1 Future work

Even though stability for this particular scenario was guaranteed thanks to the chosen control algorithms, the fact is that a higher performance could be possible by integrating the dynamics of the ground platform into the control design.

Another interesting alternative would be to integrate a prediction model in order to have a more accurate representation of the target's dynamics.

ACKNOWLEDGEMENTS

This paper was supported by the RPV project - UTC foundation and the Mexican National Council of Science and Technology - CONACyT.

REFERENCES

T. M. Cabreira, C. D. Franco, P. R. Ferreira and G. C. Buttazzo. u Energy-Aware Spiral Coverage Path Planning for UAV Photogrammetric Applications IEEE Robotics and Automation Letters, vol. 3, no. 4, pp. 3662-3668, Oct. 2018.

P. Iscold, G. A. S. Pereira and L. A. B. Torres. Development of a Hand-Launched Small UAV for Ground Reconnaissance. IEEE Transactions on Aerospace and Electronic Systems, vol. 46, no. 1, pp. 335-348, Jan. 2010.

J. Sun, B. Li, Y. Jiang, & C. Y. Wen. A camera-based target detection and positioning UAV system for search and rescue (SAR) purposes. Sensors, 16(11), 1778, (2016).

T. Oliveira, & P. Encarnação. Ground target tracking control system for unmanned aerial vehicles. Journal of Intelligent & Robotic Systems, 69(1), 373-387, (2013).

C. Wang, B. Song, P. Huang, & C. Tang. Trajectory tracking control for quadrotor robot subject to payload variation and wind gust disturbance. Journal of Intelligent & Robotic Systems, 83(2), 315-333.

A. Brezoescu, T. Espinoza, P. Castillo, and R. Lozano. Adaptive Trajectory Following for a Fixed-Wing UAV in Presence of Crosswind. J Intell Robot Syst 69, 257–271 (2013).

P. C. Garcia, R. Lozano, and A. E. Dzul. Modeling and Control of Mini-Flying Machines. Springer-Verlag, London.

M. Varga, J. C. Zufferey, Heitz, G. H. M. Zufferey, & D. Floreano. Evaluation of control strategies for fixed-wing drones following slow-moving ground agents. Robotics and Autonomous Systems, 72, 285-294, (2015).

T. Elijah, R. S. Jamisola, Z. Tjiparuro, & M. Namoshe. A review on control and maneuvering of cooperative fixed-wing drones. International Journal of Dynamics and Control, 9(3), 1332-1349, (2021).

S. Huh, & D. H. Shim. A vision-based landing system for small unmanned aerial vehicles using an airbag. Control Engineering Practice, 18(7), 812-823, (2010).

D. Zhang, & X. Wang. Autonomous Landing Control of Fixed-wing UAVs: from Theory to Field Experiment. J Intell Robot Syst 88, 619–634 (2017).

D. V. Rao, & T. H. Go. Automatic landing system design using sliding mode control. Aerospace Science and Technology, 32(1), 180-187, (2014).

T. Muskardin, G. Balmer, S. Wlach, K. Kondak, M. Laiacker, & A. Ollero. Landing of a fixed-wing uav on a mobile ground vehicle. 2016 IEEE International Conference on Robotics and Automation (ICRA) (pp. 1237-1242). IEEE. (2016, May).

M. F. Reis, R. P. Jain, A. P. Aguiar, & J. B. de Sousa. Robust moving path following control for robotic vehicles: Theory and experiments. IEEE Robotics and Automation Letters, 4(4), 3192-3199, (2019).

H. Oh, S. Kim, H. S. Shin, B. A. White, A. Tsourdos, & C. A. Rabbath. Rendezvous and standoff target tracking guidance using differential geometry. Journal of Intelligent & Robotic Systems, 69(1), 389-405, (2013).

J. B. Kuipers. Quaternions and rotation sequences: a primer with applications to orbits, aerospace, and virtual reality. Princeton university press.

J. P. Morais, S. Georgiev, & W.Sprößig. Real quaternionic calculus handbook. Springer Basel, (2014).

R. W. Beard and T. W. McLain. Small Unmanned Aircraft: Theory and Practice. 1st ed. Princeton, NJ: Princeton Univ. Press, 2012.

G. Sanahuja, FL-AIR framework, (Heudiasyc). Accessed: March 11, 2022. [online]., 2012, https://devel.hds.utc.fr/software/flair.

J. Carino, H. Abaunza, & P. Castillo. Quadrotor quaternion control. In 2015 International Conference on Unmanned Aircraft Systems (ICUAS) (pp. 825-831). IEEE, (2015, June).

A. Alatorre, P. Castillo and R. Lozano. Least Airspeed Reduction Strategy & Flight Recuperation of a Fixed-Wing Drone. 2021 International Conference on Unmanned Aircraft Systems (ICUAS), 2021, pp. 750-757.